Supporting Information

Sheh et al. 10.1073/pnas.1009017107

SI Materials and Methods

Bacteria and Animals. *H. pylori* strain SS1 was cultured on blood agar (TSA with sheep blood; Remel) or *Brucella* broth with 5% FBS under microaerobic conditions (10% H_2, 10% CO_2, 80% N_2). Specific pathogen-free (including *Helicobacter* spp.) male and female C57BL/6 *gpt* delta mice (1) bred and maintained in our facilities were used. Mice were maintained in a facility accredited by the Association for Assessment and Accreditation of Laboratory Animal Care International, housed in polycarbonate microisolator cages on hardwood bedding, and provided standard rodent chow and water ad libitum. All protocols were approved by the Massachusetts Institute of Technology Committee on Animal Care.

Experimental Design. Twenty-one 6- to 8-wk-old *gpt* delta mice (11 male and 10 female) were infected by oral gavage with 0.2 mL of *H. pylori* SS1 on alternate days for a total of three doses of approximately 1×10^8 organisms per dose (2, 3). Twelve age-matched uninfected mice were dosed with 0.2 mL of tryptic soy broth. Mice were euthanized at 6 or 12 MPI. After CO_2 asphyxiation, blood was immediately collected by cardiac puncture and the stomach and proximal duodenum were removed and incised along the greater curvature. For histopathologic study, linear gastric strips from the lesser curvature were fixed overnight in 10% neutral-buffered formalin, embedded, sectioned at 4-μm thickness, and stained with H&E. A board-certified comparative pathologist (B.H.R.), blinded to treatment groups, scored gastric lesions on an ascending scale of 0 to 4 for inflammation, epithelial defects, atrophy, hyperplasia, mucous metaplasia, hyalinosis, intestinal metaplasia, and dysplasia according to previously published criteria (4). A GHAI was calculated as the sum of scores for inflammation, epithelial defects, atrophy, hyperplasia, intestinal metaplasia, and dysplasia. Hyalinosis and mucous metaplasia were excluded from the GHAI as they have been observed to develop spontaneously in mice (4, 5). Data for two infected male mice with GHAI scores of 0 were excluded from all subsequent analyses, unless specifically noted, as a result of their lack of response to infection. The remainder of the gastric tissue was snap-frozen in liquid nitrogen and stored at −70 °C for DNA and RNA analyses.

Assay for *gpt* Mutagenesis. Fifty-seven samples from 33 mice were processed according to the *gpt* delta mutagenesis procedures to determine frequencies of point mutations (6-TG selection assay) and large deletions (Spi$^-$ assay). Animals were selected for analysis based on histopathological findings, and analyses of tissues from 15 mice were repeated two or three times to verify assay reproducibility. Animals studied at 6 MPI included five uninfected males, four uninfected females, four infected males, and four infected females; those at 12 MPI were three uninfected males, three uninfected females, four infected males, and six infected females. In the 6-TG selection assay procedure, genomic DNA was extracted from gastric tissue previously kept at −70 °C using the Recoverease DNA Isolation Kit (Stratagene). The Transpack Packaging Extract (Stratagene) was used to recover λ-EG10 phages from tissue DNA, and the 6-TG selection assay was performed as previously described (1, 6). Briefly, *E. coli* expressing Cre recombinase was infected with rescued λ-EG10 phages and incubated for 72 h on selective media containing either Cm (25 μg/mL) or Cm (25 μg/mL) plus 6-TG (25 μg/mL) to select colonies possessing Cm acetyltransferase activity only (survival) or both Cm acetyltransferase activity and loss of *gpt* function (mutant). Recovered *gpt* mutants were restreaked onto Cm and 6-TG plates for confirmation. Mutant frequency was expressed as the mutant/survivor ratio.

Confirmed 6-TG–resistant mutants were boiled and pelleted to obtain DNA template for sequencing of the *gpt* gene. A 739-bp DNA fragment containing the *gpt* gene was amplified by PCR using primers P1 (forward) 5′-TACCACTTTATCCCGCGTCAGG-3′ and primer P2 (reverse) 5′-ACAGGGTTTGGCTCAGGTTTGC-3′. PCR amplification was carried out using Vent DNA polymerase (New England Biolabs) on a DNA Engine PTC-200 (MJ Research). The reaction was started by incubation at 94 °C for 5 min, followed by 30 cycles of 30 s at 94 °C, 30 s at 56 °C, and 120 s at 72 °C and finalized by incubating at 72 °C for 5 min before storing at 4 °C (6). PCR product cleanup and DNA sequencing were performed by the Biopolymers Facility at Harvard Medical School (Boston, MA) using AMPure beads (Agencourt) and a 3730xL DNA Analyzer (Applied Biosystems) using sequencing primers A (forward) 5′-GAGGCAGTGCGTAAAAAGAC-3′ and A2 (forward) 5′-CTCGCGCAACCTATTTTCCC-3′. Sequences were aligned with the *E. coli gpt* gene (GenBank M13422.1) (7) with Geneious software (Biomatters). Mutations were individually corroborated by multiple sequence results and classified as transitions (G:C to A:T, A:T to G:C), transversions (G:C to T:A, G:C to C:G, A:T to T:A, A:T to C:G), deletions (1 bp or ≥2 bp), insertions, or complex (multiple changes). A mutation found repeated at the same site within the same sample was excluded from frequency calculations to eliminate overrepresentation caused by sibling mutations. Samples from 33 mice were sequenced. Mutation frequencies calculated for each animal and each mutation type were subjected to statistical analysis.

Spi$^-$ Assay for Large Deletions. The Spi$^-$ assay was carried out as described (1). *E. coli* strains XL-1 Blue MRA or XL-1 Blue MRA P2 lysogen were infected with phages rescued from mouse DNA and incubated for 20 min without shaking at 37 °C. The suspensions were poured on λ-trypticase agar plates (1% trypticase peptone, 0.5% NaCl, 1.2% agar), which were then incubated overnight at 37 °C to select for plaques formed in MRA P2 lawns containing phage with inactivated *red* and *gam* genes. Plaques formed in MRA lawns were counted to determine titer. Mutant phages were picked and spotted onto lawns of *E. coli* strain WL95 P2 lysogen (WL95 P2) to confirm the inactivation of *red* and *gam* genes. The mutant frequency was expressed as mutant plaque/titer ratio. *E. coli* strain LE392 was infected with recovered Spi$^-$ mutant phages to obtain phage lysates (8).

Quantitative Analysis of mRNA Expression. Total RNA was extracted from gastric tissue using TRIzol reagent (Invitrogen) and the RNeasy kit (Qiagen). cDNA was synthesized from 5 μg of total RNA with SuperScript II RT (Invitrogen). Quantitative real-time PCR was performed on cDNA using TaqMan gene expression assays (Applied Biosystems) specific for IFN-γ (assay Mm9999 9071_m1), TNF-α (Mm99999068_m1), IL-10 (Mm0043961 6_m1), IL-17 (Mm00439619_m1), iNOS (*NOS2* or *iNOS*; Mm004 40485_m1), and GAPDH (Mm99999915_g1). mRNA levels for each cytokine were normalized to the mRNA level of internal control *GAPDH* and compared with the data of uninfected mice using the $\Delta\Delta C_T$ method (User Bulletin 2; Applied Biosystems). Data were log10-transformed for analysis.

Detection of *H. pylori* Infection by Quantitative PCR. To quantify infection levels of *H. pylori* strain SS1 within the gastric mucosa, a real-time quantitative PCR assay targeting *H. pylori* urease B was used (9, 10). DNA was extracted from gastric tissue using the High Pure PCR Template purification kit (Roche). A standard curve was generated by using serial 10-fold dilutions of *H. pylori* SS1 genome copies (from 5×10^5 to 5), estimated from an average *H. pylori* genome size of 1.66 Mb (11, 12). Copy numbers of the gastric *H. pylori* genome were standardized using micrograms of murine chromosomal DNA determined by quantitative PCR using a mammalian 18S rRNA gene-based primer and probe mixture (Applied Biosystems) as described previously (13). A threshold of 15 copies of the *H. pylori* genome was set as the lower limit for a positive sample. Although five infected female mice and one infected male mouse had *H. pylori* levels under the established threshold, these mice had increased cytokine expression and higher GHAI scores consistent with that of mice infected with *H. pylori* and not uninfected mice. Despite the low counts, these six mice were considered infected during subsequent analyses as a result of serological and histological evidence. Conversely, the two mice with the highest number of *H. pylori* copies (one infected male at 6 MPI and one infected male at 12 MPI) had a GHAI of 0 and cytokine production similar to uninfected controls, indicating an aberrant response to infection, and they were excluded from subsequent analyses unless otherwise noted as a result of lack of pathology.

Serum IgG Isotype Measurement. Serum was analyzed for *H. pylori*-specific IgG2c and IgG1 by ELISA using an outer membrane protein preparation from *H. pylori* (SS1 strain) as described previously (14). In brief, 96-well flat-bottom plates were coated with 100 μL of antigen (10 μg/mL) overnight at 4 °C, and sera were diluted 1:100. Biotinylated secondary antibodies for detecting IgG2c and IgG1 were from clone 5.7 and A85-1 (BD Pharmingen). Incubation with extravidin peroxidase (Sigma-Aldrich) was followed by treatment with 2,2′-azino-bis (3-ethylbenzthiazoline-6-sulphonic acid) substrate (Kirkegaard and Perry Laboratories) for color development. Optical density was recorded on a plate reader according to the manufacturer's protocol (VersaMax; Molecular Devices).

1. Nohmi T, et al. (1996) A new transgenic mouse mutagenesis test system using Spi- and 6-thioguanine selections. *Environ Mol Mutagen* 28:465–470.
2. Fox JG, et al. (1999) High-salt diet induces gastric epithelial hyperplasia and parietal cell loss, and enhances Helicobacter pylori colonization in C57BL/6 mice. *Cancer Res* 59:4823–4828.
3. Lee A, et al. (1997) A standardized mouse model of Helicobacter pylori infection: Introducing the Sydney strain. *Gastroenterology* 112:1386–1397.
4. Rogers AB, et al. (2005) Helicobacter pylori but not high salt induces gastric intraepithelial neoplasia in B6129 mice. *Cancer Res* 65:10709–10715.
5. Kang W, Rathinavelu S, Samuelson LC, Merchant JL (2005) Interferon gamma induction of gastric mucous neck cell hypertrophy. *Lab Invest* 85:702–715.
6. Masumura K, et al. (1999) Spectra of gpt mutations in ethylnitrosourea-treated and untreated transgenic mice. *Environ Mol Mutagen* 34:1–8.
7. Nüesch J, Schümperli D (1984) Structural and functional organization of the gpt gene region of Escherichia coli. *Gene* 32:243–249.
8. Sambrook J, Fritsch EF, Maniatis T (1989) *Molecular Cloning: A Laboratory Manual* (Cold Spring Harbor Lab Press, Cold Spring Harbor, NY), 2nd Ed.
9. Fox JG, et al. (2003) Host and microbial constituents influence Helicobacter pylori-induced cancer in a murine model of hypergastrinemia. *Gastroenterology* 124: 1879–1890.
10. Maurer KJ, et al. (2006) Helicobacter pylori and cholesterol gallstone formation in C57L/J mice: A prospective study. *Am J Physiol Gastrointest Liver Physiol* 290:G175–G182.
11. Alm RA, et al. (1999) Genomic-sequence comparison of two unrelated isolates of the human gastric pathogen Helicobacter pylori. *Nature* 397:176–180.
12. Tomb JF, et al. (1997) The complete genome sequence of the gastric pathogen Helicobacter pylori. *Nature* 388:539–547.
13. Whary MT, et al. (2001) Long-term colonization levels of Helicobacter hepaticus in the cecum of hepatitis-prone A/JCr mice are significantly lower than those in hepatitis-resistant C57BL/6 mice. *Comp Med* 51:413–417.
14. Ihrig M, Whary MT, Dangler CA, Fox JG (2005) Gastric helicobacter infection induces a Th2 phenotype but does not elevate serum cholesterol in mice lacking inducible nitric oxide synthase. *Infect Immun* 73:1664–1670.

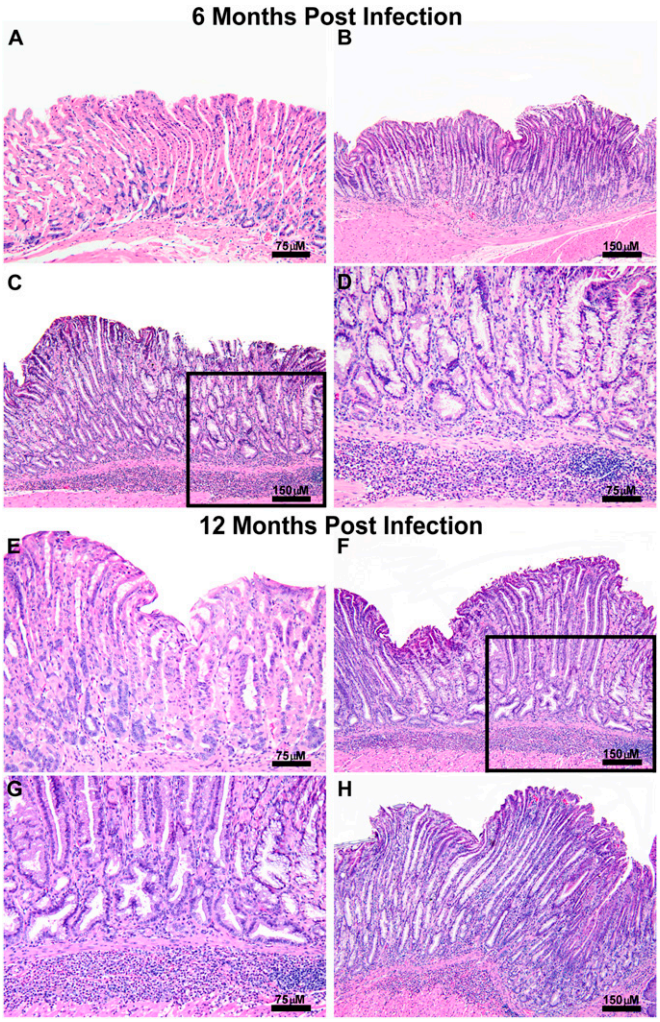

Fig. S1. *H. pylori*-infected mice display significant gastric histomorphological alterations with an accelerated development of gastric pathologic processes in females. (*A*–*D*) H&E staining of gastric tissue at 6 MPI. (*A*) Uninfected female control shows normal gastric mucosa. (*B*) *H. pylori*-infected male mice exhibiting mild gastric mucosal inflammation, associated oxyntic loss, metaplasia, and mild foveolar hyperplasia. (*C*) *H. pylori*-infected female mice had significantly higher histological activity than uninfected mice and infected males as shown by the moderate gastric inflammation, associated oxyntic loss, glandular metaplasia, prominent epithelial defects, moderate foveolar hyperplasia, and mild dysplasia. (*D*) Higher magnification of *C* shows metaplastic glands with architectural distortion and loss of orientation (dysplasia). (*E*–*H*) H&E staining of gastric tissue at 12 MPI. (*E*) Uninfected male control with minimal gastric morphological changes. (*F*) *H. pylori*-infected male with moderate inflammation, prominent oxyntic loss, hyperplasia, metaplasia, and mild dysplasia. (*G*) Higher magnification of *F* shows metaplastic and dysplastic glands. (*H*) *H. pylori*-infected female had similar gastric pathological changes as male mice. (Scale bars: 75 μM in *A*, *D*, *E*, and *G*; 150 μM in *B*, *C*, *F* and *H*.)

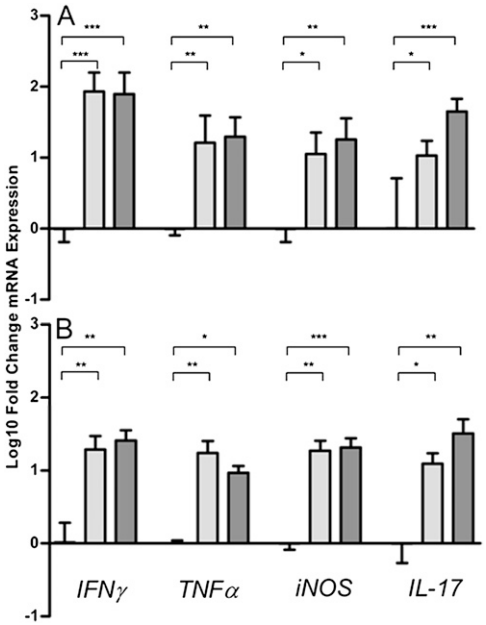

Fig. S2. *H. pylori* infection increases the expression levels of *IFNγ*, *TNFα*, *iNOS*, and *IL-17*. *IFNγ*, *TNFα*, *iNOS*, and *IL-17* transcript levels relative to *GAPDH* in the gastric mucosa are presented in male (*A*) and female (*B*) mice. Uninfected mice at 12 mo (white bars; males, $n = 3$; females, $n = 3$) and *H. pylori*-infected mice at 6 mo (light gray bars; males, $n = 4$; females, $n = 4$) and 12 mo (dark gray bars; males, $n = 5$; females, $n = 6$) are presented. *H. pylori* infection increased expression of *IFNγ*, *TNFα*, *IL-17*, and *iNOS* in both sexes at 6 and 12 mo. $*P < 0.05$, $**P < 0.01$, and $***P < 0.001$.

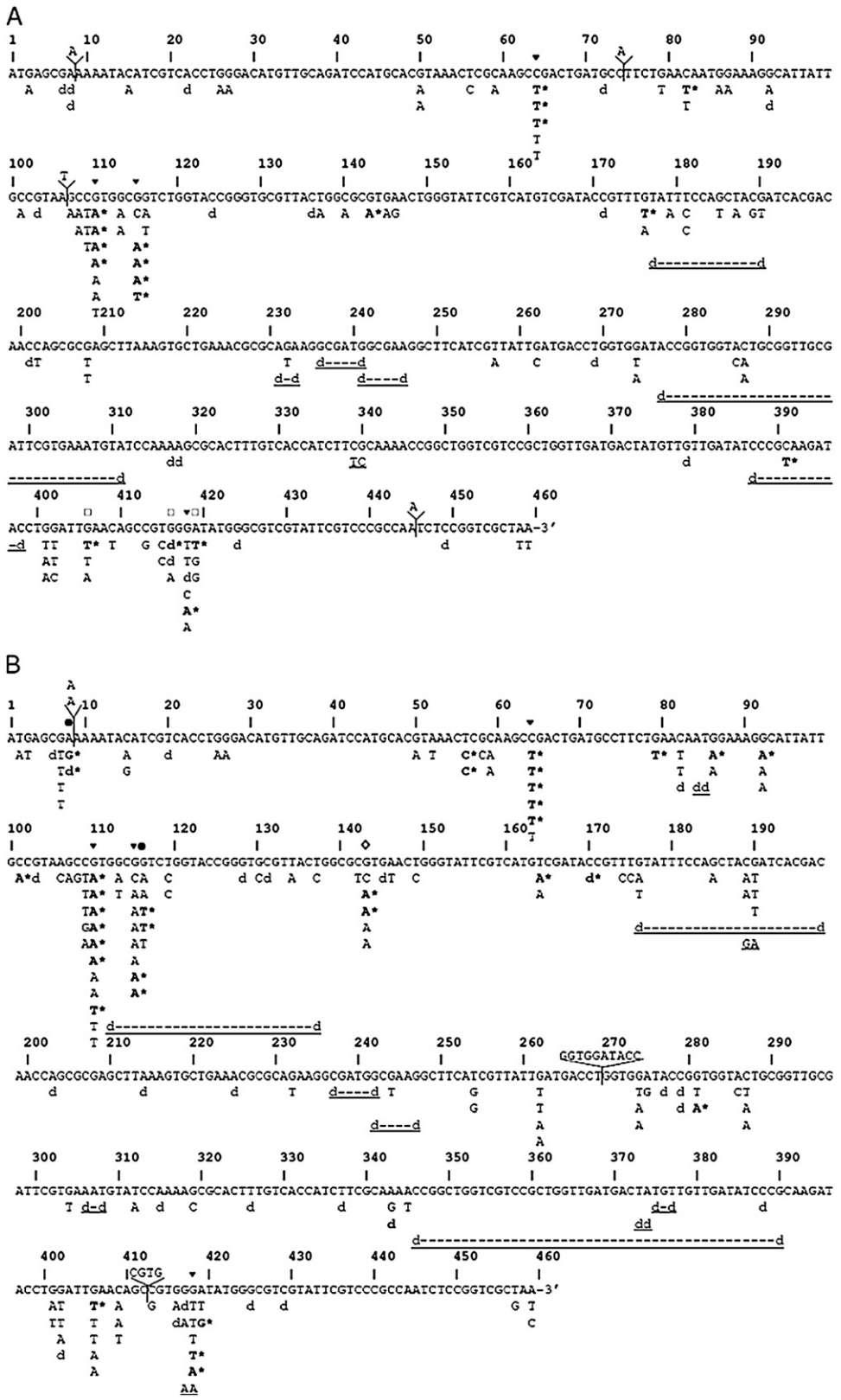

Fig. S3. *H. pylori* infection targets specific hot spots in the *gpt* gene. The distribution of mutations induced in the *gpt* gene was determined by sequencing analysis of 411 mutants. Hot spots seen in uninfected and infected mice are denoted by ▼. (*A*) Spectra of all uninfected mice. Not shown is a complex mutation from 407 to 429. A hot spot mainly seen in uninfected males is marked by □. (*B*) Spectra of all infected mice. Not shown is a complex mutation from 389 to 419. Mutations at 142 and 174 were second mutations. Hot spots mainly seen in infected mice of both sexes are represented by ◇ and hot spots seen mostly in infected females are marked ●. N* represents 3× mutations, d represents a deletion. Underlined mutations denote a single mutation.

Table S1. Number of A:T-to-G:C transitions and G:C-to-T:A transversions in *H. pylori*–infected female mice at 12 MPI is higher than in other groups

	6 mo			12 mo		
Effect	Uninfected all (n = 6)	Infected male (n = 4)	Infected female (n = 8)	Uninfected all (n = 14)	Infected male (n = 5)	Infected female (n = 11)
Transition						
G:C to A:T	32 (50.0)	7 (43.8)	35 (42.7)	41 (41.4)	16 (48.5)	39 (33.3)
A:T to G:C	2 (3.1)	0	4 (4.9)	6 (6.1)	1 (3.0)	15 (12.8)
Transversion						
G:C to T:A	11 (17.2)	5 (31.3)	16 (19.5)	21 (21.2)	7 (21.2)	31 (26.5)
G:C to C:G	2 (3.1)	1 (6.3)	3 (3.7)	4 (4.0)	3 (9.1)	2 (1.7)
A:T to T:A	4 (6.3)	0	6 (7.3)	5 (5.1)	0	6 (5.1)
A:T to C:G	0	1 (6.3)	3 (3.7)	1 (1.0)	0	2 (1.7)
Deletion						
1-bp deletion	10 (15.6)	2 (12.5)	8 (9.8)	12 (12.1)	4 (12.1)	15 (12.8)
≥2-bp deletion	1 (1.6)	0	4 (4.9)	5 (5.1)	1 (3.0)	4 (3.4)
Insertion	0	0	2 (2.4)	4 (4.0)	0	2 (1.7)
Complex mutation	2 (3.1)	0	1 (1.2)	0	1 (3.0)	1 (0.9)
Total	64 (100)	16 (100)	82 (100)	99 (100)	33 (100)	117 (100)

Values in parentheses are percentages. The number of A:T-to-G:C transitions and G:C-to-T:A transversions was elevated in female mice infected with *H. pylori* for 12 mo. The number of mutations was determined from the sequence analysis of 411 mutants recovered from the *gpt* assay after excluding 155 mutants considered siblings. Control mice of both sexes were grouped for this analysis.